ORIGINAL ARTICLE

Divergent growth responses to warming and drying climates between native and non-native tree species in Northeast China

Lining Song[1,2,3] · Jiaojun Zhu[1,2,3] · Jinxin Zhang[1,2,3] · Kai Wang[4] · Linyou Lü[5] · Fengbai Wang[5] · Guochen Wang[6]

Abstract

Key message **Increased intrinsic water use efficiency enhances tree growth of native species, but not that of non-native species under warming and drying climates in Northeast China.**

Abstract Climate change significantly affects forest ecosystems. However, little is known about whether non-native and native tree species show similar responses to global warming. We found different trends in the basal area increment (BAI) and tree-ring stable carbon isotope ratio ($\delta^{13}C$) of two non-native (*Pinus sylvestris* var. *mongolica* and *Populus × xiaozhuanica*) and two native (*Pinus tabuliformis* and *Ulmus pumila*) tree species during the warming and drying periods from 1985 to 2014. The BAI of non-native tree species was stable, whereas that of the native tree species exhibited a significant increase. A significant increase in tree-ring $\delta^{13}C_{corr}$ (corrected for atmospheric changes in $\delta^{13}C$) for non-native tree species indicated increasing water stress. The intrinsic water use efficiency (iWUE, derived from tree-ring $\delta^{13}C$) of both non-native and native tree species increased significantly. However, the magnitude of the increase in iWUE was higher in non-native tree species than in native tree species, indicating that non-native tree species suffered stronger water stress. Increasing iWUE but no increase in BAI for non-native tree species suggested that water stress reduced stomatal conductance and, consequently, reduced carbon uptake. In contrast, increased iWUE accompanied by an enhanced BAI for native tree species indicated an increase in photosynthetic capacity induced by CO_2 fertilization. These findings suggest that non-native tree species would experience greater mortality under extreme drought conditions once water stress passes a physiological threshold. However, native tree species would suffer only slightly due to benefiting from CO_2 fertilization.

Keywords Tree ring · Carbon isotope composition · Water stress · Dieback

✉ Jiaojun Zhu
jiaojunzhu@iae.ac.cn

1 CAS Key Laboratory of Forest Ecology and Management, Institute of Applied Ecology, Shenyang 110016, China

2 Qingyuan Forest CERN, Chinese Academy of Sciences, Shenyang 110016, China

3 Liaoning Key Laboratory for Management of Non-commercial Forests, Shenyang 110016, China

4 College of Environmental Sciences and Engineering, Liaoning Technical University, Fuxin 123000, China

5 Liaoning Institute of Sandy Land Control and Utilization, Fuxin 123000, China

6 Liaoning Institute of Sand-Fixation and Afforestation Research, Fuxin 123000, China

Introduction

Water is the most important limiting factor for tree growth and survival in arid and semiarid regions (Cao et al. 2011). Climate models predict that most arid and semiarid regions will experience warming and drying conditions, especially in Northeast China (IPCC 2013; Wang et al. 2016). Consequently, increasing water stress is expected to have negative impacts on tree growth and physiological status (Altieri et al. 2015). As shown by recent studies, global-change-induced drought is associated with forest dieback and mortality worldwide (Anderegg et al. 2013; Zhang et al. 2017; Song et al. 2017), altering the composition, structure and biogeography of forests (Allen et al. 2010; Walker et al. 2015). Therefore, it is essential to investigate the response of trees to climate variations (especially changes in water availability) (Battipaglia et al. 2009; Pellizzari et al. 2016), which contributes to the understanding of the mechanisms

of drought-induced mortality and the prediction of altered vegetation dynamics in arid and semiarid regions (Barbeta et al. 2015; Song et al. 2016; Feichtinger et al. 2017; Zhang et al. 2018).

Trees respond to environmental changes (e.g., changes in water availability) by adjusting their stomatal conductance and photosynthetic assimilation rates, which translate into changes in growth (Feichtinger et al. 2017; Martínez-Sancho et al. 2017). These adjustments at the tree level interact with and influence the transpiration and carbon assimilation rates from the stand level to the landscape level (Levesque et al. 2017). Long-term data about physiological and environmental processes at annual time scales can be obtained through features such as tree-ring width and stable carbon isotope composition (δ^{13}C) (McCarroll and Loader 2004). Tree-ring width is an invaluable indicator for inferring tree radial growth over long periods, from decades to centuries, which has been widely applied to study the responses of trees to environmental changes (Martin-Benito et al. 2017). Moreover, the stable carbon isotope composition (δ^{13}C) in tree rings is the result of discrimination against the heavier $^{13}CO_2$ during carboxylation and diffusion through the stomata, which are linearly related to the ratio of intercellular and atmospheric CO_2 (C_i/C_a) during the period in which the carbon was fixed (Farquhar et al. 1982; Farquhar et al. 1989). Therefore, tree-ring δ^{13}C has been widely used to reflect the balance between the assimilation rate and the stomatal conductance or intrinsic water use efficiency (iWUE) (Dawson et al. 2002).

The temporal dynamics in iWUE depend largely on water availability through its influence on the stomatal regulation of gas exchange in arid and semiarid regions (Warren et al. 2001; Ferrio et al. 2003), which can be used to assess how stomatal conductance and photosynthesis respond to changes in the soil water availability. Therefore, standard dendrochronological methods combined with a carbon isotope analysis offer a physiologically based tool to reveal the long-term growth and ecophysiology of tree responses to changes in the water availability (Newberry 2010; Silva et al. 2010). Although most studies have focused on the response of different tree species to drought in arid and semiarid regions (Anderegg et al. 2013; Brito et al. 2016; Song et al. 2017), little attention has been given to comparisons of the responses of non-native and native tree species to changes in water availability, especially in semiarid sandy regions.

The Keerqin Sandy Land is one of the most severe desertification areas in Northeast China (Song et al. 2015, 2016). To control the spread of desertification, a variety of non-native tree species, e.g., *Pinus sylvestris* var. *mongolica* (*P. mongolica*) and *Populus* spp., have been planted, as well as native tree species, such as *Pinus tabuliformis* (*P. tabuliformis*) and *Ulmus pumila* (*U. pumila*), in the Keerqin Sandy Land since the 1950s (Jiang et al. 2002). Although these non-native tree species were selected for drought tolerance, dieback often occurs in some non-native tree species, such as *P. mongolica* and *Populus × xiaozhuanica* (*P. xiaozhuanica*), during extreme drought years (Zhu et al. 2008; Song et al. 2016). In contrast, native trees (*P. tabuliformis* and *U. pumila*) rarely suffer from such problems under the same water conditions (Jiang et al. 2002; Jiao 2006). The causes of such growth differences between the non-native and native tree species remain unclear. Previous studies have indicated that water deficiency was the main reason for the dieback of non-native tree species (Zhu et al. 2006, 2008; Song et al. 2016). However, the previous studies were short term. Knowledge about the long-term growth and ecophysiological responses of trees (e.g., water use efficiency) to changes in water availability is still lacking, especially regarding the differences between non-native and native tree species. This lack of knowledge confines our understanding of the mechanisms underlying the dieback of non-native tree species in semiarid sandy land.

To determine the differences in tree growth and intrinsic water use efficiency responses to global warming between non-native and native tree species growing in a semiarid sandy region of China, radial growth (basal area increment, BAI) and tree-ring carbon isotope composition (δ^{13}C) in two non-native tree species (*P. mongolica* and *P. xiaozhuanica*) and two native tree species (*P. tabuliformis* and *U. pumila*) over the past 30 years (1985–2014) were measured and compared in combination with observations of environmental factors (air temperature, precipitation, the Palmer Drought Severity Index and the groundwater level). The objectives of this study were to (1) determine the differences in BAI and iWUE (calculated from tree-ring δ^{13}C) between the non-native and native tree species and (2) clarify how the non-native and native tree species respond to changes in the water availability based on the BAI and iWUE. This study contributes to understanding the mechanism underlying non-native tree species dieback and provides insight for forest management in semiarid sandy regions.

Materials and methods

Study site

This study was conducted in the Zhanggutai region (42°35′–42°47′N, 122°23′–122°40′E, 226 m a.s.l.), Liaoning Province, China, which is located in the southeastern part of Keerqin Sandy Land (Fig. 1a). This region belongs to the semiarid climatic zone. The mean annual temperature is approximately 6.7 °C, with minimum and maximum air temperatures of −29.5 °C and 37.2 °C, respectively. The mean annual precipitation is 478 mm (1954–2015), and approximately 67% of rainfall occurs between June and August.
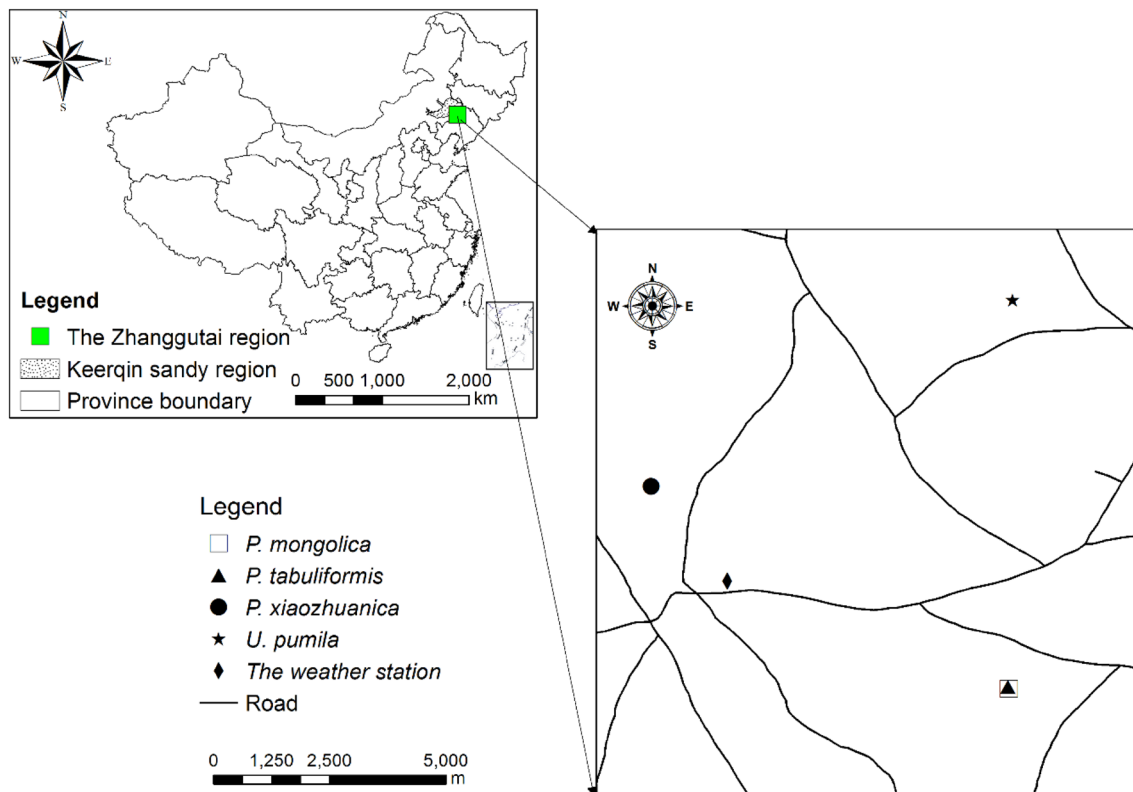
Fig. 1 Locations of the study region (**a**) and tree-ring sample sites (**b**)

The mean pan evaporation is approximately 1700 mm. The growing season comprises the months from April to October (Jiang et al. 2002). The major soil type is classified as belonging to the Semiaripsamment taxonomic group, which is developed from sandy parent material through the action of wind (Zhu et al. 2008). The soil salinity, soil texture, and soil structures were distributed homogeneously in the study region (Zhu et al. 2007). The groundwater level is approximately 5.0 m at present (Song et al. 2016). Tree species in the study region included *P. sylvestris* var. *mongolica*, *Populus*×*xiaozhuanica*, *P. tabuliformis*, and *U. pumila*. *P. sylvestris* var. *mongolica* and *P. tabuliformis* belong to the genus *Pinus*, whereas *Populus*×*xiaozhuanica* and *U. pumila* belong to the genera *Populus* and *Ulmus*, respectively. The understory was composed of annual herbaceous plant species. Three geomorphological features were present in the study area: dunes, low aeolian land and gentle sand slopes.

Sampling

In March 2015, two non-native (*P. mongolica* and *P. xiaozhuanica*) and two native (*P. tabuliformis* and *U. pumila*) tree species were selected for sampling. The *P. mongolica* and *P. tabuliformis* samples came from the same site, whereas *P. xiaozhuanica* and *U. pumila* were sampled

from different sites. The distance between the sampling sites of *P. mongolica* (or *P. tabuliformis*) and *U. pumila* was approximately 8.4 km, while the distance between the sampling sites of *P. mongolica* (or *P. tabuliformis*) and *P. xiaozhuanica* was approximately 7.1 km (Fig. 1b). There had been no logging activity during the past 30 years for any of the studied tree species in the study sites. The ages of the studied tree species were over 50 years in 2015, except for *P. xiaozhuanica*, whose age was over 40 years. According to standard dendrochronological methods, 19, 16, 17 and 16 trees of *P. mongolica*, *P. xiaozhuanica*, *P. tabuliformis*, and *U. pumila* were sampled, respectively (Table 1). Additionally, the diameter at breast height and the height of the sampled trees were measured (Table 1). For each sampled tree, two cores (north and south) were extracted at breast height (approximately 1.3 m above ground) using 5.15 mm diameter increment borers.

Tree-ring width measurement and basal area increment calculation

The core samples were dried, mounted, and surfaced with progressively finer grade sandpaper until the rings were visible. Cores were visually cross-dated under a binocular microscope. The core samples were then measured with

Table 1 Statistics of developed tree-ring width chronologies

Origin	Tree species	Tree no.	DBH (cm)	Height (m)	Mean RW (mm year^{-1})	Mean BAI (cm^2 year^{-1})	Autocorr[a]	MS[a]	SD[a]	SNR[a]	EPS[a]
Non-native	*P. mongolica*	19	28.2±0.5	10.2±0.3	3.2	19.2	0.68	0.24	0.32	78.55	0.99
	P. xiaozhuanica	16	34.0±1.0	20.2±0.8	3.7	29.3	0.64	0.20	0.32	10.80	0.92
Native	*P. tabuliformis*	17	20.1±0.6	7.5±0.2	2.2	13.5	0.71	0.31	0.41	79.76	0.99
	U. pumila	16	36.5±1.9	10.5±0.4	3.7	29.5	− 0.01	0.37	0.33	17.52	0.95

DBH diameter at breast height, *RW* ring width, *BAI* basal area increment, *autocorr* first-order autocorrelation, *MS* mean sensitivity, *SD* standard deviation, *SNR* signal-to-noise ratio, *EPS* expressed population signal

[a]Calculated on the basis of standardized chronologies

a precision of 0.001 mm using LINTAB 6 measurement equipment (Frank Rinn, Heidelberg, Germany) fitted with a Leica MS5 stereoscope and were analyzed with the TSAP software package (Frank Rinn, Heidelberg, Germany). The COFECHA program was used to control the quality of the cross-dating (Holmes 1983). Then, all of the tree-ring series were detrended to remove the non-climatic signals and to maximize the climatic information in the series using a negative exponential function or linear curves in the ARSTAN program. Several descriptive statistics commonly used in dendrochronology were also calculated (Table 1). The higher first-order autocorrelation values for *P. mongolica*, *P. xiaozhuanica* and *P. tabuliformis* indicated that the radial growth of these tree species was most strongly influenced by conditions in the preceding year (Table 1). The mean sensitivity values ranged from 0.20 to 0.37, which indicated that the tree-ring widths for the studied tree species were sufficiently sensitive to climatic variability (Table 1). All of the expressed population signal (EPS) values of the studied tree species exceeded the suggested threshold of 0.85 (Wigley et al. 1984), indicating a strong climate signal in chronologies, which was also supported by high signal-to-noise ratio values (Table 1). The raw tree-ring width (TRW) was converted into basal area increment (BAI) to remove variations in radial growth that are attributable to increasing circumference according to the following formula (Silva et al. 2010):

$$\mathrm{BAI} = \pi(R_n^2 - R_{n-1}^2), \tag{1}$$

where R is the radius of the tree inside the bark and n is the year of the tree-ring formation. BAI was used as a surrogate for tree growth (Linares and Camarero 2012). To examine the mean growth trend, the BAI in the same year for all individuals in each tree species was averaged. The BAI data were not standardized to preserve the long-term growth rate over the study period (Tiwari et al. 2017).

Carbon isotope composition measurement

After dating and ring width measurements, six trees (two cores per tree) of each species with similar growth trends were

selected for isotopic analysis. The sampled cores were stripped from the channelled wood, and then the surfaces of the tree core samples were cleaned by means of an ultrasonic bath to remove remaining wood dust and glue (Schollaen et al. 2015). To prevent and weaken juvenile effects on isotopic tree-ring signatures, only the past 30 years (1985–2014) of ring formation were sampled for each species. Under a binocular microscope, the wood cores were carefully cut year by year using a razor blade. Several recent studies have tested and proven the representativeness of the pooled isotopic series for the tree-ring δ^{13}C compared to individual isotopic series (Szymczak et al. 2012; Lu et al. 2018). Therefore, the material from the annual ring of six trees for each species in each year was pooled and ground in a ball mill. Stable isotope analysis was performed without further cellulose extraction in the present study because cellulose extraction is not required for tree-ring δ^{13}C analysis (Gori et al. 2013; Jansen et al. 2013), and most recent research has shown that whole wood might be a better integrator for climatic signals than cellulose (Weigt et al. 2015; Brito et al. 2016). Homogenized wood samples transferred into tin capsules were combusted (carbon) using a Thermo-Finnigan Flash HT elemental analyser. Sample gas was flushed via a ConFlo III into a Delta V Advantage isotope ratio mass spectrometer (Thermo-Scientific, Bremen, Germany). The isotopic values are expressed in delta notation (in ‰ units) relative to VPDB (Vienna Pee Dee Belemnite). Repeated measurements of laboratory standards revealed a measurement precision better than 0.1‰.

$$\delta^{13}\mathrm{C} \ (\text{‰}) = (R_{\text{sample}}/R_{\text{standard}} - 1) \times 1000, \tag{2}$$

where R_{sample} and R_{standard} represent the ^{13}C/^{12}C ratios of the sample and the VPDB international standard, respectively (Farquhar et al. 1982).

Intrinsic water use efficiency (iWUE) calculation

The tree-ring δ^{13}C was corrected for the progressive decline in atmospheric δ^{13}C by calculating ^{13}C discrimination (Δ^{13}C):

$$\Delta^{13}C = (\delta^{13}C_{atm} - \delta^{13}C_{sample})/[1 + (\delta^{13}C_{sample}/1000)], \tag{3}$$

where $\delta^{13}C_{atm}$ and $\delta^{13}C_{sample}$ are the $^{13}C/^{12}C$ ratios in the atmospheric CO_2 and in the tree rings, respectively. Following Farquhar et al. (1982), the iWUE was calculated using the following equation:

$$iWUE = A/g = C_{atm}(b - \Delta^{13}C)/[1.6(b - a)], \tag{4}$$

where A is the rate of net photosynthesis, g stomatal conductance to H_2O, C_a the ambient air CO_2 concentration, 1.6 the ratio between the diffusivities of water vapor and CO_2 in the air, a the diffusion fractionation across the boundary layer and the stomata (4.4‰), and b is the Rubisco enzymatic biologic fractionation (27.0‰). The long-term C_{atm} and atmospheric $\delta^{13}C$ from 1985 to 2003 were obtained from McCarroll and Loader (2004). The atmospheric $\delta^{13}C$ for 2004–2014 was estimated by the near-linear decline in atmospheric $\delta^{13}C$ over the last decades (Song et al. 2017). C_{atm} data (2004–2014) were obtained from Mauna Loa observatory (available online at http://www.esrl.noaa.gov/gmd/obop/mlo/).

Environmental data

Annual air temperature and precipitation during 1985–2014 were obtained from the Zhanggutai weather station (Fig. 1b). To reflect the moisture status of the study region, annual Palmer Drought Severity Index (PDSI) data from 1985 to 2014 were obtained from the KNMI Climate Explorer (available online at http://climexp.knmi.nl/). A value of PDSI below zero indicates a moisture deficit. The groundwater level data were collected from Zheng et al. (2012) and Song et al. (2017).

Statistical analyses

The raw $\delta^{13}C$ data were corrected for the decline in $\delta^{13}C$ in atmospheric CO_2 due to fossil fuel emissions following the method of McCarroll and Loader (2004) (henceforth referred to as $\delta^{13}C_{corr}$) as below:

$$\delta^{13}C_{corr} = \delta^{13}C_{sample} - (\delta^{13}C_{atm} + 6.4). \tag{5}$$

The significant temporal trends in environmental factors, TRW, BAI, $\delta^{13}C_{corr}$ and iWUE, were analyzed using regression analyses. ANCOVA was used to test for significant differences among regression lines in temporal trends of tree-ring $\delta^{13}C_{corr}$ and iWUE for the studied tree species. Correlation analyses between BAI and iWUE were performed to investigate how the changes in iWUE affected tree growth. The correlations between the tree-ring index and the monthly climatic variables (temperature and precipitation) from August of the previous year until

August of the current year were calculated using Dendro-Clim 2002 software (Biondi and Waikul 2004). Additionally, to investigate the relationships between the tree-ring $\delta^{13}C_{corr}$, iWUE, BAI and environmental variables (temperature, precipitation and PDSI), all annual series were detrended using the first differences (one year minus the previous year) method (Battipaglia et al. 2009). Linear regression analysis was performed using the first-differenced data. The ANCOVA was used to test for significant differences among regression lines between tree-ring $\delta^{13}C_{corr}$, iWUE, BAI and environmental variables for the studied tree species. All of the statistical calculations and analyses were conducted using the SPSS software package (Version 16.0, SPSS. Inc., Chicago, IL, USA).

Results

Climate and groundwater level

The annual mean air temperature increased from 5.3 °C in 1985 to 8.7 °C in 2014 and showed a statistically significant increase during the past 30 years (1985–2014) (Fig. 2a). The annual precipitation during the past 30 years ranged between 285.9 and 772.6 mm, and revealed no statistically significant long-term trend (Fig. 2b). The growing season PDSI varied from − 3.7 to 3.6 and showed a significant decrease over the past 30 years (Fig. 2c). The groundwater level decreased significantly from 3.8 m in 1985 to 5.2 m in 2014, at a rate of 0.05 m per year (Fig. 2d). These results indicate warming and drying trends over the past 30 years in the study region.

Tree-ring width and basal area increment

The two non-native tree species (*P. mongolica* and *P. xiaozhuanica*) and two native (*P. tabuliformis* and *U. pumila*) tree species showed different annual variations in tree-ring width (TRW) and basal area increment (BAI) over the past 30 years (1985–2014) (Fig. 3). The TRW of the two non-native tree species showed a significant decrease over the past 30 years, but no significant changes in TRW were observed for the two native tree species (Fig. 3a). However, when the TRW was converted into BAI, the BAI of the two non-native tree species showed no significant changes over the past 30 years, whereas the BAI of the two native tree species exhibited a significant increase (Fig. 3b). The mean BAI of *P. mongolica* and *P. xiaozhuanica* was 19.2 and 29.3 cm^2 year^{-1}, respectively, whereas the mean BAI was 13.5 and 29.5 cm^2 year^{-1} for *P. tabuliformis* and *U. pumila*, respectively (Table 1).
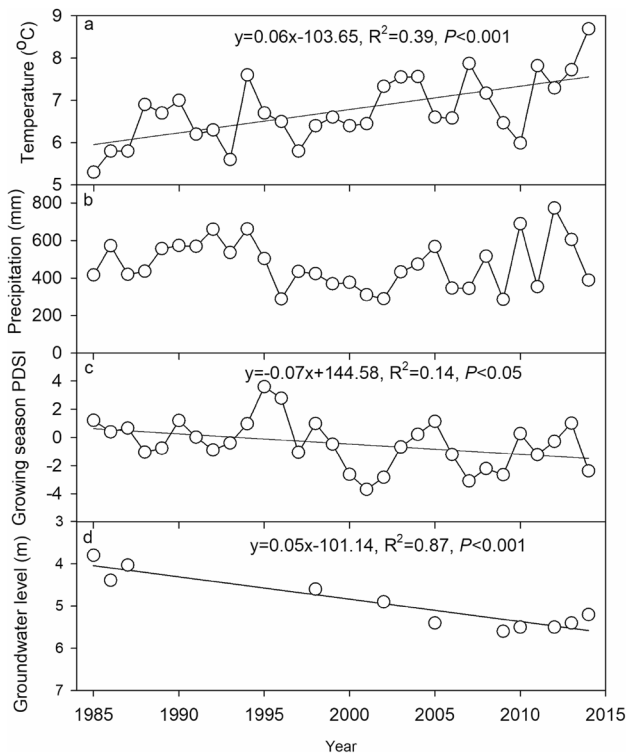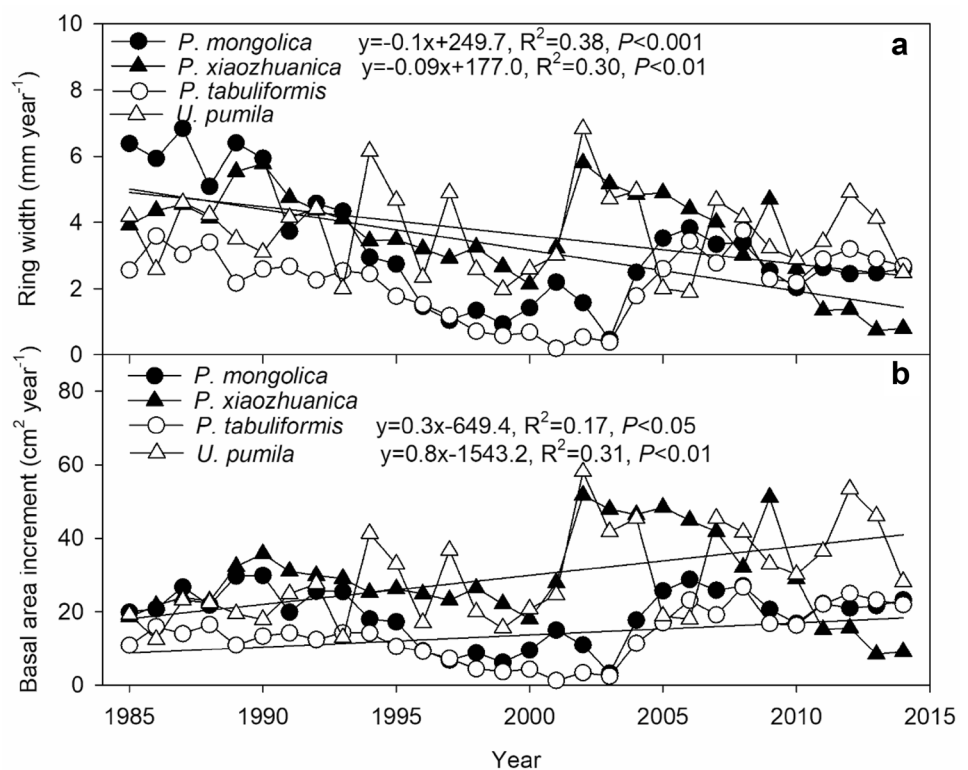
Fig. 2 Temporal variation in annual mean temperature (**a**), annual precipitation (**b**), growing season PDSI (**c**) and groundwater level (**d**) in the study region over the past 30 years (1985–2014)

Tree-ring δ¹³C$_{corr}$ and iWUE

The tree-ring $\delta^{13}C_{corr}$ ranged from -24.84 to $-23.6‰$ and from -26.58 to $-24.86‰$ for *P. mongolica* and *P. xiaozhuanica*, respectively, with mean values of $-23.45‰$ and $-25.62‰$. However, the tree-ring $\delta^{13}C_{corr}$ varied between -25.13 and $-23.36‰$ for *P. tabuliformis* and between -26.53 and $-25.51‰$ for *U. pumila*, with mean values of $-24.15‰$ and $-26.08‰$ (Fig. 4a). In addition, tree-ring $\delta^{13}C_{corr}$ exhibited a significant increase for *P. mongolica*, *P. xiaozhuanica* and *U. pumila* over the past 30 years (1985–2014), but the magnitude of the increase in tree-ring $\delta^{13}C_{corr}$ was higher in *P. mongolica* and *P. xiaozhuanica* than in *U. pumila* (Fig. 4a, ANCOVA, $F = 3.3$, $P < 0.05$). In contrast, no significant trend in tree-ring $\delta^{13}C_{corr}$ was found for *P. tabuliformis* (Fig. 4a).

Intrinsic water use efficiency (iWUE, calculated from tree-ring $\delta^{13}C$) ranged from 82.46 to 118.11 μmol mol⁻¹ for *P. mongolica* and from 65.26 to 91.09 μmol mol⁻¹ for *P. xiaozhuanica*, with mean values of 101.96 μmol mol⁻¹ and 79.80 μmol mol⁻¹, whereas the iWUE varied between 88.14 and 107.88 μmol mol⁻¹ and between 65.92 and 84.36 μmol mol⁻¹ for *P. tabuliformis* and *U. pumila*, respectively, with mean values of 94.65 μmol mol⁻¹ and 74.96 μmol mol⁻¹ (Fig. 4b). Additionally, iWUE exhibited a significant increase for all of the studied tree species over the past 30 years. The magnitude of the increase in iWUE during 1985–2014 for *P. mongolica* and *P. xiaozhuanica* was

Fig. 3 Temporal variations in tree-ring width (**a**) and basal area increment (**b**) for the non-native and native tree species over the past 30 years (1985–2014)

Fig. 4 Temporal variations in tree-ring carbon isotope composition ($\delta^{13}C_{corr}$, **a**) and intrinsic water use efficiency (iWUE, **b**) for the non-native and native tree species over the past 30 years (1985–2014)
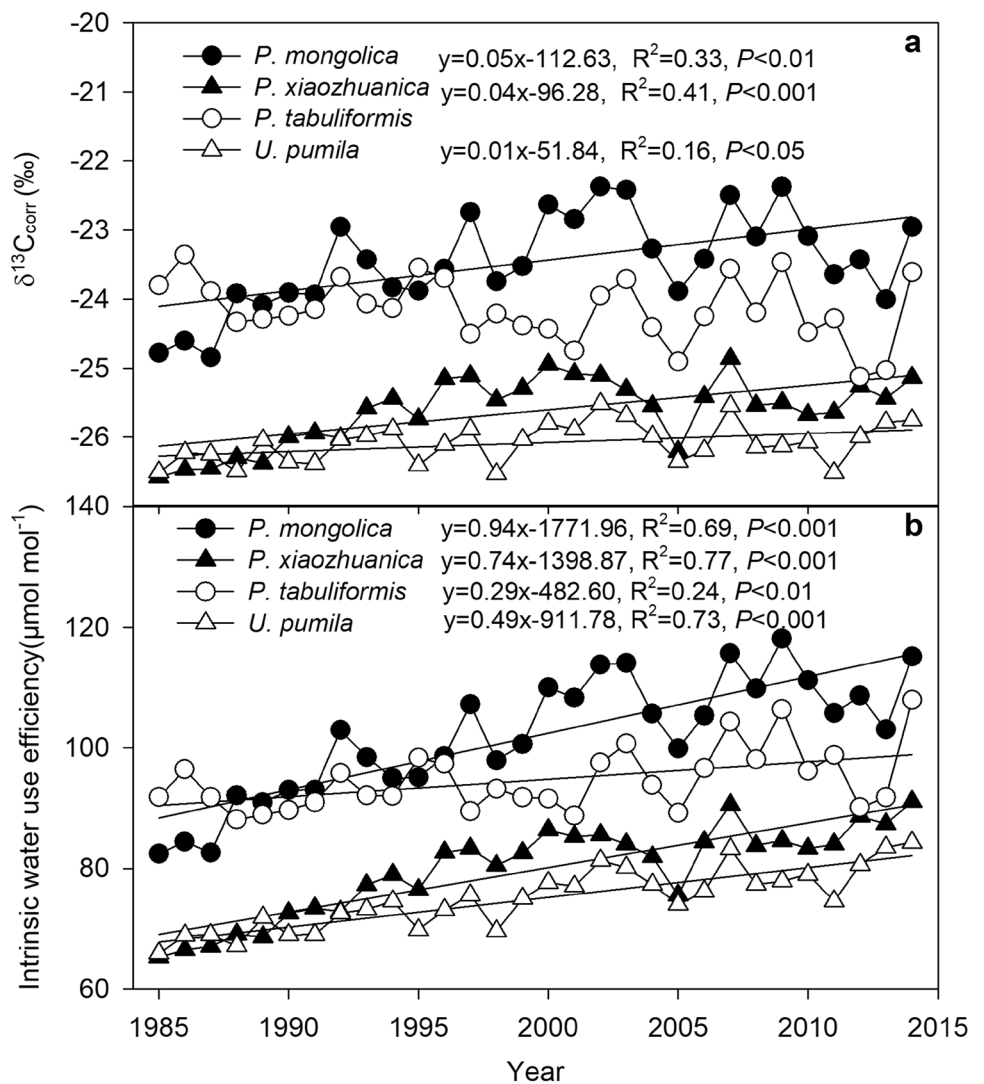
42.1% and 42.8%, respectively, whereas it was only 17.5% and 29.5% for *P. tabuliformis* and *U. pumila*, respectively (Fig. 4b). Furthermore, changes in iWUE over time differed among the studied tree species, with higher slope responses in *P. mongolica* and *P. xiaozhuanica* than in *P. tabuliformis* and *U. pumila* (Fig. 4b, ANCOVA, $F = 9.8$, $P < 0.001$).

Relationships between iWUE and BAI and between tree-ring index and climate

A significant positive relationship between iWUE and BAI was observed for *U. pumila*, but there were no significant relationships between iWUE and BAI for the other tree species (Fig. 5).

The tree-ring index for *P. mongolica* was positively correlated with the temperature in August and October of the previous year, whereas it was negatively correlated with the temperature in November of the previous year (Fig. 6a). In addition, the tree-ring index for *P. mongolica* was positively
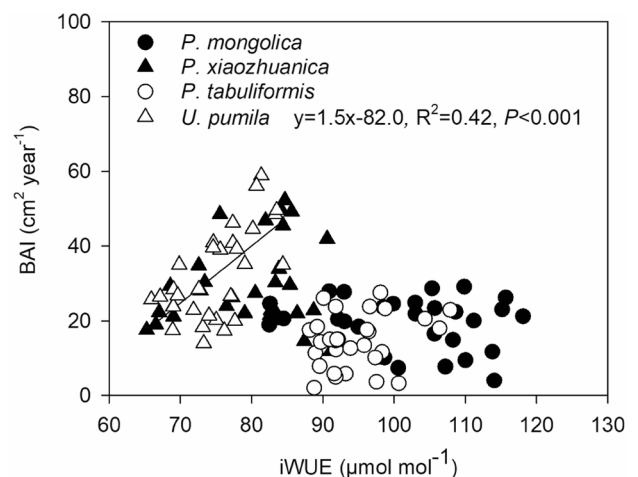

Fig. 5 Basal area increment (BAI) relationships with intrinsic water use efficiency (iWUE) for the non-native and native tree species

correlated with precipitation in September of the previous year and February of the current year (Fig. 6b). For *P. xiaozhuanica*, the tree-ring index was negatively correlated with temperature in January, February, June, July and August of the current year and negatively correlated with precipitation in October of the previous year (Fig. 6). However, the tree-ring index for *P. tabuliformis* was positively correlated with the temperature in October of the previous year and August of the current year, and was positively correlated with precipitation in February of the current year (Fig. 6). The tree-ring index for *U. pumila* was positively correlated with temperature in April and July of the current year, whereas it was negatively correlated with precipitation in October of the previous year (Fig. 6).

Tree-ring δ¹³C$_{corr}$, iWUE and BAI relationships with annual mean temperature, precipitation and growing season PDSI

There was a significant positive relationship between detrended tree-ring $\delta^{13}C_{corr}$ and detrended temperature, and a negative relationship between detrended tree-ring $\delta^{13}C_{corr}$ and detrended precipitation for *P. tabuliformis* (Fig. 7a, b). In addition, significant negative relationships between detrended tree-ring $\delta^{13}C_{corr}$ and detrended PDSI were found for *P. mongolica, P. xiaozhuanica* and *U. pumila* (Fig. 7c). However, the slope of detrended tree-ring $\delta^{13}C_{corr}$ against detrended PDSI was higher in *P. mongolica* and

P. xiaozhuanica than in *U. pumila* (ANCOVA, $F = 4.7$, $P < 0.05$).

A significant positive relationship between the detrended temperature and detrended iWUE, and a negative relationship between detrended precipitation and detrended iWUE were observed for *P. tabuliformis* (Fig. 7d, e). Additionally, significant negative relationships between detrended PDSI and detrended iWUE were found for *P. mongolica* and *P. xiaozhuanica* (Fig. 7f).

There was a significant positive relationship between the detrended temperature and detrended BAI for *U. pumila* (Fig. 7g), whereas no significant relationships between the detrended BAI and detrended temperature, precipitation or PDSI were observed for the other tree species (Fig. 7g–i).

Discussion

Differences in tree growth between non-native and native tree species

Significant differences in the basal area increment (BAI) patterns between two non-native and two native tree species suggest that the ecophysiological mechanism response to warming and drying differed among the studied tree species. The constant BAI over time of non-native tree species (Fig. 3b) indicates that the growth of the non-native tree species had been limited by some stress factors during the

Fig. 6 Correlations of tree-ring index with temperature (**a**) and precipitation (**b**) for the non-native and native tree species over the past 30 years (1985–2014). Asterisks indicate $P < 0.05$
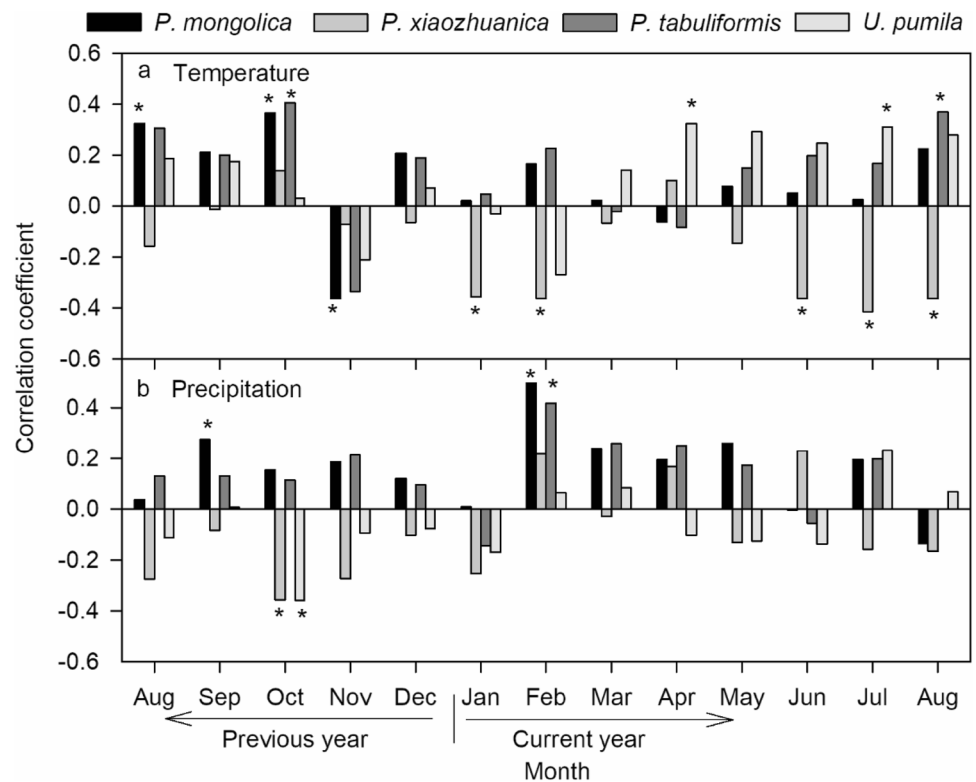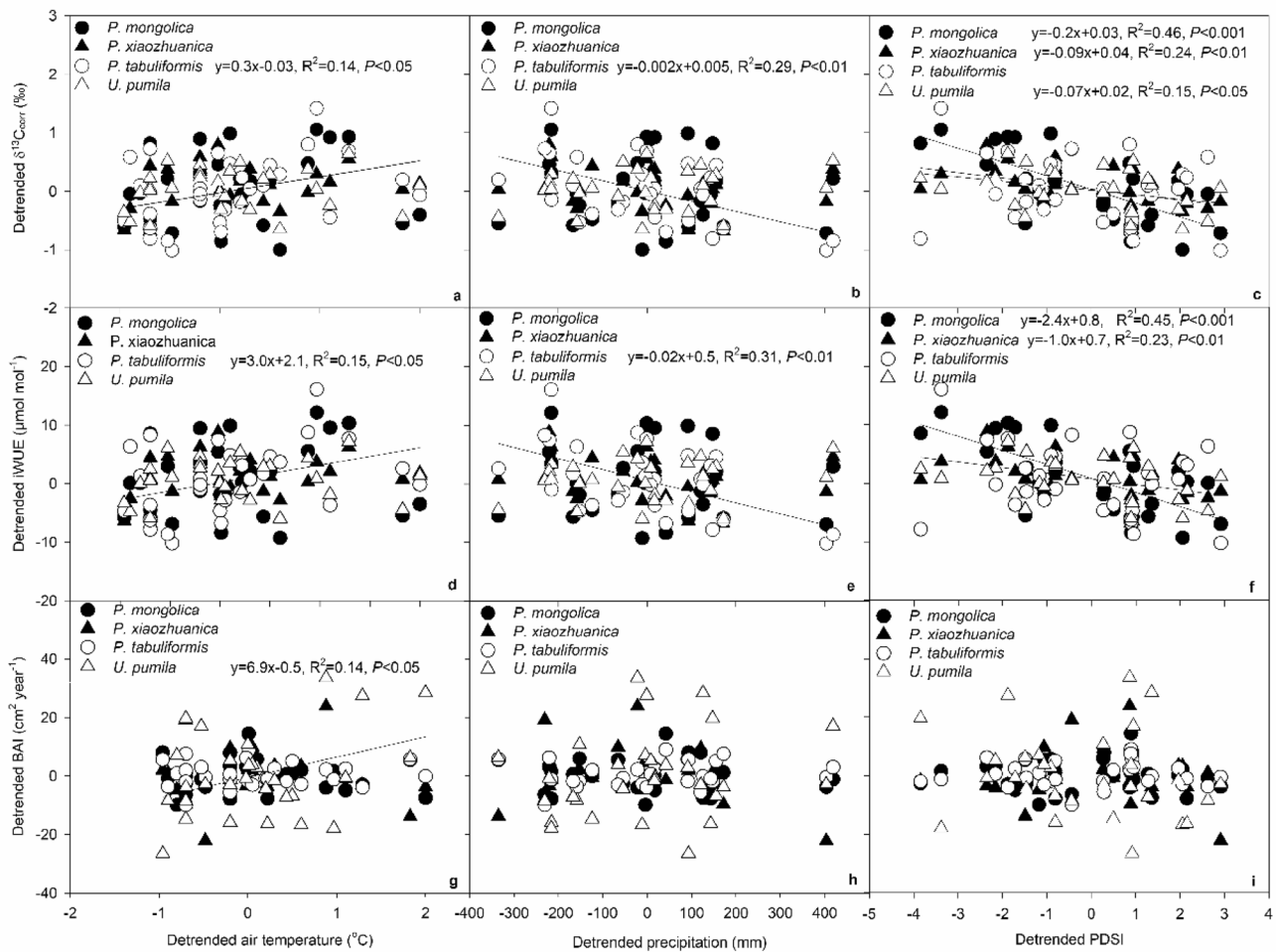
Fig. 7 Tree-ring carbon isotope composition ($\delta^{13}C_{corr}$), intrinsic water use efficiency (iWUE) and basal area increment (BAI) relationships with annual mean temperature (**a**, **d**, **g**), annual precipitation (**b**, **e**, **h**) and growing season PDSI (**c**, **f**, **i**)

last 30 years, which offset the expected CO_2 fertilization effect (Peñuelas et al. 2011; van der Sleen et al. 2015). Since the atmospheric CO_2 concentration is increasing, forests should theoretically display increased growth as a result of the CO_2 fertilization effect (Wang et al. 2012; Drake et al. 2017; Zhang et al. 2018). In fact, most studies have suggested that tree growth has not been stimulated as expected in response to the CO_2 increase and it has thus remained stable or even declined in some areas, which indicates that other factors (e.g., drought stress) offset or override the expected CO_2 fertilization effect (Martínez-Vilalta et al. 2008; Linares and Camarero 2012). In the present study, although no responses of BAI to temperature, precipitation and PDSI were observed for the non-native tree species (Fig. 7), a significant increase in the tree-ring $\delta^{13}C_{corr}$ and its sensitivity to PDSI (Figs. 4a, 7c) indicate that the non-native tree species suffered from increasing water stress induced by drying, thus leading to limited growth. The $\delta^{13}C$ of plants has been widely used as a proxy for water

stress because plants discriminate less against ^{13}C when under stress (Oltean et al. 2016). When water availability decreases, stomatal conductance is known to be reduced to minimize water loss, thus leading to an increase in tree-ring $\delta^{13}C$ (Feichtinger et al. 2017). This was also partly supported by a significant negative relationship between the tree-ring index and temperature during winter (January and February) and summer (June, July and August) for *P. xiaozhuanica* (Fig. 6a). High temperatures, especially in the summer, increase evapotranspiration, thereby exacerbating water stress; high temperatures are often associated with reduced tree growth (Battipaglia et al. 2009). In addition, in the study region, groundwater has been an important water source for tree growth (Jiang et al. 2002). For example, Song et al. (2016) reported that *P. mongolica* had to utilize groundwater in addition to soil water after approximately 30 years of growth, and groundwater was the primary water source for pine trees during the years of extremely low rainfall in the study region. Gao et al. (2013) reported that 11-year-old

Populus spp. utilized both soil water and groundwater during the growing season in sandy land. However, the groundwater level has significantly declined over the past 30 years (Fig. 2d). Therefore, the decreasing groundwater level may also contribute to water stress for non-native tree species such as *P. mongolica* and *P. xiaozhuanica*. Conversely, the increasing BAI with time for the native tree species suggests that the CO_2 fertilization effect on growth has overridden the concomitant negative effects of the environmental stressors (Granda et al. 2014). This finding was consistent with an expected growth increase under elevated CO_2 concentration since photosynthesis was stimulated and thus led to enhanced carbon uptake (Urrutia-Jalabert et al. 2015). For example, Lu et al. (2018) reported that *Platycladus orientalis* increased its growth over time, suggesting that the growth of *P. orientalis* benefited from the elevated atmospheric CO_2 concentrations in the semiarid region of China. In the present study, an increase in BAI with time for the native tree species may be associated not only with increasing tree size and age (Stephenson et al. 2014) but also with enhanced photosynthetic capacity accompanied by an increased atmospheric CO_2 concentration. In addition, the elevated temperature also contributed to boosting growth for the native tree species (Way and Oren 2010; Peñuelas et al. 2011; Flexas et al. 2012; Zhang et al. 2018). This was demonstrated by significant positive relationships between the tree-ring index and temperature in October of the previous year and in August for *P. tabuliformis* and in April and July for *U. pumila* (Fig. 6a). Similar to our findings, Peñuelas and Filella (2001) suggested that accelerated tree growth throughout Europe is caused by global warming.

Differences in intrinsic water use efficiency (iWUE) between non-native and native tree species

The non-native and native tree species increased their iWUE over the past 30 years, and the magnitude of the increase in iWUE ranged from 17.5 to 42.8%, which was within the iWUE increase range observed around the world (Wang et al. 2012; Brito et al. 2016; Huang et al. 2017; Lu et al. 2018). For example, Granda et al. (2014) reported that the iWUE of *Quercus faginea*, *Pinus nigra* and *Juniperus thurifera* in forests of central Spain increased by 18.6%, 21.3% and 15.0%, respectively, from the 1970s to the 2000s. Hietz et al. (2005) found that the iWUE increased 34% for *Cedrela odorata* L. and 52% for *Swietenia macrophylla* King in Brazil. Many studies have reported the increasing trend of iWUE in different forests around the world during recent decades (Peñuelas et al. 2011; Silva and Anand 2013; Frank et al. 2015).

We found that the magnitudes of the increase in iWUE with time for the non-native tree species (42.1% and 42.8% for *P. mongolica* and *P. xiaozhuanica*, respectively) were

significantly higher than those for the native tree species (17.5% for *P. tabuliformis* and 29.5% for *U. pumila*) (Fig. 4b). Since the iWUE is the ratio of the carbon assimilation rate to the stomatal conductance for water vapor, a higher iWUE increase could be due to either greater carbon assimilation in response to increased atmospheric CO_2 or lower stomatal conductance in response to water stress (Silva et al. 2010). However, atmospheric CO_2 has increased similarly at all of the sampling sites, and the higher increase in the iWUE for the non-native tree species compared with the native tree species seems attributable to reduced water availability and corresponding stronger water stress (Peñuelas et al. 2011; Song et al. 2017). This was also supported by a steeper slope of increase in tree-ring $\delta^{13}C_{corr}$ for the non-native tree species compared with the native tree species (Fig. 4a). Similar results have been reported in other regions. For example, González-Muñoz et al. (2015) reported a higher increase in the iWUE for exotic trees than for native tree species in inner Spain riparian forests, suggesting that the exotic trees suffered from higher drought stress. In the present study, the higher increase in the iWUE for non-native tree species compared with native tree species is likely to result from higher climatic sensitivity of the iWUE for non-native tree species (i.e., the response to PDSI in the non-native tree species) (Fig. 7f).

Relationships between iWUE and BAI for the non-native and native tree species

The increased iWUE for the non-native tree species did not translate into increased radial growth (Figs. 3b, 4b), which agreed with previous findings of increases in the iWUE but no increases (or even a decrease) in the tree radial growth (Linares and Camarero 2012; Gómez-Guerrero et al. 2013; van der Sleen et al. 2015). Generally, tree growth (BAI) has not increased as the atmospheric CO_2 and iWUE have increased, which suggests that other factors (e.g., warming-induced stress) have stimulated stomatal closure and consequently reduced carbon uptake and growth, over-riding the potential CO2 fertilization effect (Peñuelas et al. 2011; Silva and Anand 2013; Lévesque et al. 2014). Therefore, our results suggest that water stress-induced stomatal closure resulting from warming and drying has prevented the non-native species from taking advantage of the increased atmospheric CO_2 for faster growth.

In contrast to the non-native tree species, we found that the native tree species significantly increased their radial growth (BAI) over the last 30 years (Fig. 3b), which is associated with increasing iWUE (Fig. 4b) and suggests that an increment in the photosynthetic rate induced by the increasing atmospheric CO_2 concentration overrides a decrease in stomatal conductance by warming and drying (Tognetti et al. 2014). The growth of native tree species increased as

the iWUE increased in the semiarid sandy region of China, possibly due to high drought tolerance and high temperature resistance (Zhang et al. 2005; Hu and Wang 2015). Although the responses of tree-ring $\delta^{13}C_{corr}$ and iWUE to temperature and precipitation for *P. tabuliformis* and of tree-ring $\delta^{13}C_{corr}$ to PDSI for *U. pumila* were observed, no response of tree-ring $\delta^{13}C_{corr}$ and iWUE to PDSI for *P. tabuliformis* (Fig. 7c, f) and the positive response of BAI to temperature for *U. pumila* (Fig. 7g) partly supported our explanation.

In addition, the absence of relationships between BAI and iWUE for *P. mongolica*, *P. xiaozhuanica* and *P. tabuliformis* (Fig. 5) may be because tree growth is often disconnected from carbon assimilation caused by variable allocation to other tissues and remobilization of carbohydrate reserves (Urrutia-Jalabert et al. 2015). Moreover, increases in temperature also induce higher rates of photorespiration, which would lower the net primary productivity and thus contribute to BAI disconnecting from carbon assimilation (Peñuelas et al. 2011).

Conclusions

In this study, the standard dendrochronological methods combined with a carbon isotope analysis were used to study the BAI and iWUE of the non-native and native tree species in response to warming and drying in the semiarid sandy land. Divergent growth and intrinsic water use efficiency responses to warming and drying climates between native and non-native tree species were found. The iWUE increased, but the lack of increase in BAI for the non-native tree species suggests that water stress reduced stomatal conductance and, consequently, reduced carbon uptake. In contrast, increased iWUE accompanied by enhanced BAI for the native tree species indicates that an increase in the photosynthetic capacity induced by elevated levels of atmospheric CO_2 overrode a decrease in the stomatal conductance by warming and drying, and thus increased carbon uptake. These findings suggest that non-native tree species such as *P. mongolica* and *P. xiaozhuanica* would be more susceptible to dieback under extreme drought years once water stress passes a physiological threshold, whereas the native tree species (e.g., *P. tabuliformis* and *U. pumila*) would suffer only slightly because they benefit from CO_2 fertilization in the semiarid sandy land. Consequently, forest management for relieving water stress (e.g., thinning and maintaining a stable groundwater level) will be necessary to protect the increasingly vulnerable forests of non-native tree species, such as *P. mongolica* and *P. xiaozhuanica,* in the semiarid sandy region.

Author contribution statement LS: writing the paper and running the data analysis. JZ: designing the experiment and writing the paper. JZ and KW: running the data analysis. LL, WF and WG: sampling in the field.

Compliance with ethical standards

Conflict of interest The authors declare that they have no conflict of interest.

References

Allen CD, Macalady AK, Chenchouni H, Bachelet D, McDowell N, Vennetier M et al (2010) A global overview of drought and heat induced tree mortality reveals emerging climate change risks for forests. For Ecol Manag 259:660–684

Altieri S, Mereu S, Cherubini P, Castaldi S, Sirignano C, Lubritto C, Battipaglia G (2015) Tree-ring carbon and oxygen isotopes indicate different water use strategies in three Mediterranean shrubs at Capo Caccia (Sardinia, Italy). Trees 29:1593–1603

Anderegg WRL, Kane JM, Anderegg LDL (2013) Consequences of widespread tree mortality triggered by drought and temperature stress. Nat Clim Change 3(1):30–36

Barbeta A, Mejía-Chang M, Ogaya R, Voltas J, Dawson TE, Peñuelas J (2015) The combined effects of a long-term experimental drought and an extreme drought on the use of plant–water sources in a Mediterranean forest. Glob Change Biol 21(3):1213–1225

Battipaglia G, Saurer M, Cherubini P, Siegwolf RTW, Cotrufo MF (2009) Tree rings indicate different drought resistance of a native (*Abies alba* Mill.) and a nonnative (*Picea abies* (L.) Karst.) species co-occurring at a dry site in Southern Italy. For Ecol Manag 257:820–828

Biondi F, Waikul K (2004) DENDROCLIM2002: a C++ program for statistical calibration of climate signals in tree-ring chronologies. Comput Geosci 30:303–311

Brito P, Grams TEE, Matyssek R, Jimenez MS, Gonzalez-Rodríguez AM, Oberhuber W, Wieser G (2016) Increased water use efficiency does not prevent growth decline of *Pinus canariensis* in a semi-arid treeline ecotone in Tenerife, Canary Islands (Spain). Ann For Sci 73:741–749

Cao SX, Chen L, Shankman D, Wang CM, Wang XB, Zhang H (2011) Excessive reliance on afforestation in China's arid and semi-arid regions: lessons in ecological restoration. Earth Sci Rev 104:240–245

Dawson TE, Mambelli S, Plamboeck AH, Tempter PH, Tu KP (2002) Stable isotopes in plant ecology. Annu Rev Ecol Syst 33:507–559

Drake BL, Hanson DT, Lowrey TK, Sharp ZD (2017) The carbon fertilization effect over a century of anthropogenic CO_2 emissions: higher intracellular CO_2 and more drought resistance among

invasive and native grass species contrasts with increased water use efficiency for woody plants in the US Southwest. Glob Change Biol 23:782–792

Farquhar GD, O'Leary MH, Berry JA (1982) On the relationship between carbon isotope discrimination and the intercellular carbon dioxide concentration in leaves. Aust J Plant Physiol 9:121–137

Farquhar GD, Ehleringer JR, Hubick KT (1989) Carbon isotope discrimination and photosynthesis. Annu Rev Plant Physiol Plant Mol Biol 40:503–537

Feichtinger LM, Siegwolf RTW, Gessler A, Buchmann N, Lévesque M, Rigling A (2017) Plasticity in gas-exchange physiology of mature Scots pine and European larch drive short- and long-term adjustments to changes in water availability. Plant Cell Environ 40(9):1972–1983

Ferrio JP, Florit A, Vega A, Serrano L, Voltas J (2003) Δ^{13}C and tree-ring width reflect different drought responses in *Quercus ilex* and *Pinus halepensis*. Oecologia 137:512–518

Flexas J, Loreto F, Medrano H (2012) Terrestrial photosynthesis in a changing environment: a molecular, physiological, and ecological approach. Cambridge University Press, Cambridge

Frank DC, Poulter B, Saurer M, Esper J, Huntingford C, Helle G et al (2015) Water-use efficiency and transpiration across European forests during the Anthropocene. Nat Clim Change 5:579–583

Gao C, Lu SW, Li SN, Yang XB, Chen B, Kong LW (2013) Strategy of water utilization for Poplar plantation based on isotope and stem sap flow. J Irrig Drain 32(6):108–112 **(in Chinese with English abstract)**

Gómez-Guerrero A, Silva LCR, Barrera-Reyes M, Kishchuk B, Velázquez-Martínez A, Martínez-Trinidad T, Plascencia-Escalante FO, Horwath WR (2013) Growth decline and divergent tree ring isotopic composition (δ^{13}C and δ^{18}O) contradict predictions of CO_2 stimulation in high altitudinal forests. Glob Change Biol 19(6):1748–1758

González-Muñoz N, Linares JC, Castro-Díez P, Sass-Klaassen U (2015) Contrasting secondary growth and water-use efficiency patterns in native and exotic trees co-occurring in inner Spain riparian forests. For Syst 24:e017

Gori Y, Wehrens R, Greule M, Keppler F, Ziller L, La Porta N, Camin F (2013) Carbon, hydrogen and oxygen stable isotope ratios of whole wood, cellulose and lignin methoxyl groups of *Picea abies* as climate proxies. Rapid Commun Mass Spectrom 27(1):265–275

Granda E, Rossatto DR, Camarero JJ, Voltas J, Valladares F (2014) Growth and carbon isotopes of Mediterranean trees reveal contrasting responses to increased carbon dioxide and drought. Oecologia 174:307–317

Hietz P, Wanek W, Dunisch O (2005) Long-term trends in cellulose δ^{13}C and water-use efficiency of tropical Cedrela and Swietenia from Brazil. Tree Physiol 25:745–752

Holmes RL (1983) Computer-assisted quality control in tree-ring dating and measurement. Tree Ring Bull 43:68–78

Hu WJ, Wang H (2015) Drought resistance of three superior species. Prot For Sci Technol 3:12–13 **(in Chinese with English abstract)**

Huang R, Zhu HF, Liu XH, Liang EY, Grießinger J, Wu GJ, Li XX, Bräuning A (2017) Does increasing intrinsic water use efficiency (iWUE) stimulate tree growth at natural alpine timberline on the southeastern Tibetan Plateau? Glob Planet Change 148:217–226

IPCC (2013) Climate Change 2013: the physical science basis. Contribution of Working Group I to the Fifth Assessment Report of the Intergovernmental Panel on Climate Change. Cambridge University Press, Cambridge

Jansen K, Sohort J, Kohnle U, Ensminger I, Gessler A (2013) Tree ring isotopic composition, radial increment and height growth reveal provenance-specific reactions of Douglas-fir towards environmental parameters. Trees 27(1):37–52

Jiang FQ, Cao CY, Zeng DH, Guan WB, Wu XY, Zheng YR (2002) Degradation and restoration of ecosystems on Keerqin sandy land. China Forestry Publishing House, Beijing **(in Chinese)**

Jiao SR (2006) Influence of extreme climatic condition on exotic tree species in Horqin sandy land. Prot For Sci Technol 6:15–17 **(in Chinese with English abstract)**

Levesque M, Andreu-Hayles L, Pederson N (2017) Water availability drives gas exchange and growth of trees in northeastern US, not elevated CO_2 and reduced acid deposition. Sci Rep 7:46158

Lévesque M, Siegwolf R, Saurer M, Eilmann B, Rigling A (2014) Increased water-use efficiency does not lead to enhanced tree growth under xeric and mesic conditions. New Phytol 203:94–109

Linares JC, Camarero JJ (2012) From pattern to process: linking intrinsic water use efficiency to drought-induced forest decline. Glob Change Biol 18:1000–1015

Lu WW, Yu XX, Jia GD, Li HZ, Liu ZQ (2018) Responses of intrinsic water-use efficiency and tree growth to climate change in semi-arid areas of North China. Sci Rep 8(1):308

Martin-Benito D, Anchukaitis KJ, Evans MN, delRío M, Beeckman H, Cañellas I (2017) Effects of drought on xylem anatomy and water-use efficiency of two co-occurring pine species. Forests 8:332

Martínez-Sancho E, Dorado-Liñán I, Gutiérrez Merino E, Matiu M, Helle G, Heinrich I, Menzel A (2017) Increased water-use efficiency translates into contrasting growth patterns of Scots pine and sessile oak at their southern distribution limits. Glob Change Biol 24(3):1012–1028

Martínez-Vilalta J, López BC, Adell N, Badiella L, Ninyerola M (2008) Twentieth century increase of Scots pine radial growth in NE Spain shows strong climate interactions. Glob Change Biol 14:2868–2881

McCarroll D, Loader NJ (2004) Stable isotopes in tree rings. Quat Sci Rev 23:771–801

Newberry TL (2010) Effect of climatic variability on δ^{13}C and tree-ring growth in piñon pine (*Pinus edulis*). Trees 24:551–559

Oltean GS, Comeau PG, White B (2016) Carbon isotope discrimination by *Picea glauca* and *Populus tremuloides* is related to the topographic depth to water index and rainfall. Can J For Res 46(10):1225–1233

Pellizzari E, Camarero JJ, Gazol A, Sangüesa-Barreda G, Carrer M (2016) Wood anatomy and carbon-isotope discrimination support long-term hydraulic deterioration as a major cause of drought-induced dieback. Glob Change Biol 22:2125–2137

Peñuelas J, Filella I (2001) Phenology: responses to a warming world. Science 294:793–795

Peñuelas J, Canadell JG, Ogaya R (2011) Increased water-use efficiency during the 20th century did not translate into enhanced tree growth. Glob Ecol Biogeogr 20(4):597–608

Schollaen K, Baschek H, Heinrich I, Helle G (2015) Technical Note: an improved guideline for rapid and precise sample preparation of tree-ring stable isotope analysis. Biogeosci Discuss 12:11587–11623

Silva LCR, Anand M (2013) Probing for the influence of atmospheric CO_2 and climate change on forest ecosystems across biomes. Glob Ecol Biogeogr 22(1):83–92

Silva LCR, Anand M, Leithead MD (2010) Recent widespread tree growth decline despite increasing atmospheric CO_2. PLoS One 5(7):e11543

Song LN, Zhu JJ, Yan QL, Li MC, Yu GQ (2015) Comparison of intrinsic water use efficiency between different aged *Pinus sylvestris* var. *mongolica* wide windbreaks in semiarid sandy land of northern China. Agroforest Syst 89(3):477–489

Song LN, Zhu JJ, Li MC, Zhang JX (2016) Water use patterns of *Pinus sylvestris* var. *mongolica* trees of different ages in a semiarid sandy lands of Northeast China. Environ Exp Bot 129:94–107

Song LN, Li MC, Zhu JJ, Zhang JX (2017) Comparisons of radial growth and tree-ring cellulose δ^{13}C for *Pinus sylvestris* var. *mongolica* in natural and plantation forests on sandy lands. J For Res 22(3):160–168

Stephenson NL, Das AJ, Condit R, Russo SE, Baker PJ, Beckman NG et al (2014) Rate of tree carbon accumulation increases continuously with tree size. Nature 507(7490):90–93

Szymczak S, Joachimski MM, Bräuning A, Kuhlemann A (2012) Are pooled tree ring δ^{13}C and δ^{18}O series reliable climate archives?—a case study of *Pinus nigra* spp. laricio (Corsica/France). Chem Geol 308–309:40–48

Tiwari A, Fan ZX, Jump AS, Zhou ZK (2017) Warming induced growth decline of Himalayan birch at its lower range edge in a semi-arid region of Trans-Himalaya, central Nepal. Plant Ecol 218(5):621–633

Tognetti R, Lombardi F, Lasserre B, Cherubini P, Marchetti M (2014) Tree-ring stable isotopes reveal twentieth-century increases in water-use efficiency of *Fagus sylvatica* and *Nothofagus* spp. in Italian and Chilean mountains. PLoS One 9:e113136

Urrutia-Jalabert R, Malhi Y, Barichivich J, Lara A, Delgado-Huertas A, Rodríguez CG, Cuq E (2015) Increased water use efficiency but contrasting tree growth patterns in *Fitzroya cupressoides* forests of southern Chile during recent decades. J Geophys Res Biogeosci 120:2505–2524

van der Sleen P, Groenendijk P, Vlam M, Anten NPR, Boom A, Bongers F, Pons TL, Terburg G, Zuidema PA (2015) No growth stimulation of tropical trees by 150 years of CO_2 fertilization but water-use efficiency increased. Nat Geosci 8(1):24–28

Walker X, Mack MC, Johnstone JF (2015) Stable carbon isotope analysis reveals widespread drought stress in boreal black spruce forests. Glob Change Biol 21:3102–3113

Wang WZ, Liu XH, An WL, Xu GB, Zeng XM (2012) Increased intrinsic water-use efficiency during a period with persistent decreased tree radial growth in northwestern China: causes and implications. For Ecol Manag 275:14–22

Wang LY, Yuan X, Xie ZH, Wu PL, Li YH (2016) Increasing flash droughts over China during the recent global warming hiatus. Sci Rep 6:30571

Warren CR, McGrath JF, Adams MA (2001) Water availability and carbon isotope discrimination in conifers. Oecologia 127:476–486

Way DA, Oren R (2010) Differential responses to changes in growth temperature between trees from different functional groups and biomes: a review and synthesis of data. Tree Physiol 30:669–688

Weigt RB, Bräunlich S, Zimmermann L, Saurer M, Grams TEE, Dietric HP, Siegwolf RTW, Nikolova PS (2015) Comparison of δ^{18}O and δ^{13}C values between tree-ring whole wood and cellulose in five species growing under two different site conditions. Rapid Commun Mass Spectrom 29:2233–2244

Wigley TM, Briffa KR, Jones PD (1984) On the average value of correlated time series, with applications in dendroclimatology and hydrometeorology. J Clim Appl Meteorol 23:201–213

Zhang JY, Dan F, Wei ZZ, Zhao HL, Zhang TH (2005) Determination of the ability of several tree and shrub species to endure and survive extreme aridity with methods of limited areas under field condition in Horqin sand Land. Acta Ecol Sin 26(2):467–473 **(in Chinese with English abstract)**

Zhang Q, Shao M, Jia X, Wei X (2017) Relationship of climatic and forest factors to drought- and heat-induced tree mortality. PLoS One 12(1):e0169770

Zhang XW, Liu XH, Zhang QL, Zeng XM, Xu GB, Wu GJ, Wang WZ (2018) Species-specific tree growth and intrinsic water-use efficiency of Dahurian larch (*Larix gmelinii*) and Mongolian pine (*Pinus sylvestris* var. *mongolica*) growing in a boreal permafrost region of the Greater Hinggan Mountains, Northeastern China. Agric For Meteorol 248:145–155

Zheng X, Zhu JJ, Yan QL, Song LN (2012) Effects of land use changes on the groundwater table and the decline of *Pinus sylvestris* var. *mongolica* plantations in southern Horqin Sandy Land, Northeast China. Agric Water Manag 109:94–106

Zhu JJ, Kang HZ, Tan H, Xu ML (2006) Effects of drought stresses induced by polyethylene glycol on germination of *Pinus sylvestris* var. *mongolica* seeds from natural and plantation forests on sandy land. J For Res 11(5):319–328

Zhu JJ, Kang HZ, Gonda Y (2007) Application of Wenner configuration to estimate soil water content in pine plantations on sandy land. Pedosphere 17(6):801–812

Zhu JJ, Li FQ, Xu ML, Kang HZ, Xu DY (2008) The role of ectomycorrhizal fungi in alleviating pine decline in semiarid sandy soil of northern China: an experimental approach. Ann For Sci 65:1–12

Publisher's Note Springer Nature remains neutral with regard to jurisdictional claims in published maps and institutional affiliations.